



HAL
open science

Fingerprinting sediment sources in the outlet reservoir of a hilly cultivated catchment in Tunisia

Abir Ben Slimane, Damien Raclot, O. Evrard, Mustapha Sanaa, Irène Lefevre, Mehdi Ahmadi, Mouna Tounsi, Cornelia Rumpel, Abdallah Ben Mammou, Yves Le Bissonnais

► **To cite this version:**

Abir Ben Slimane, Damien Raclot, O. Evrard, Mustapha Sanaa, Irène Lefevre, et al.. Fingerprinting sediment sources in the outlet reservoir of a hilly cultivated catchment in Tunisia. *Journal of Soils and Sediments*, 2013, 13 (4), pp.801-815. 10.1007/s11368-012-0642-6 . cea-02615650

HAL Id: cea-02615650

<https://cea.hal.science/cea-02615650>

Submitted on 23 May 2020

HAL is a multi-disciplinary open access archive for the deposit and dissemination of scientific research documents, whether they are published or not. The documents may come from teaching and research institutions in France or abroad, or from public or private research centers.

L'archive ouverte pluridisciplinaire **HAL**, est destinée au dépôt et à la diffusion de documents scientifiques de niveau recherche, publiés ou non, émanant des établissements d'enseignement et de recherche français ou étrangers, des laboratoires publics ou privés.

1 SEDIMENTS, SEC 3 • HILLSLOPE AND RIVER BASIN SEDIMENT DYNAMICS •

2 RESEARCH ARTICLE

3

4 **Fingerprinting sediment sources in the outlet reservoir of a hilly cultivated catchment of**
5 **Tunisia**

6
7
8
9 **Abir Ben Slimane • Damien Raclot • Olivier Evrard • Mustapha Sanaa • Irène Lefèvre •**
10 **Mehdi Ahmadi • Mouna Tounsi • Cornelia Rumpel • Abdallah Ben Mammou • Yves le**
11 **Bissonnais**

12 A. Ben Slimane • M. Sanaa

13 Institut National Agronomique de Tunisie, 43, Avenue Charles Nicolle 1082, Tunis-
14 Mahrajène, Tunisia

15
16 A. Ben Slimane • D. Raclot (✉)

17 IRD-UMR LISAH(INRA-IRD-Supagro), 2 Place Viala, 34060 Montpellier, France

18 e-mail: damien.raclot@ird.fr

19
20 O. Evrard • I. Lefèvre • M. Ahmadi

21 Laboratoire des Sciences du Climat et de l'Environnement (LSCE/IPSL) – Unité Mixte de
22 Recherche 8212 (CEA, CNRS, UVSQ), 91198 Gif-sur-Yvette Cedex, France

23
24 M. Tounsi • A. Ben Mammou

25 Laboratoire des Ressources Minérales et Environnement, Département de Géologie, Faculté
26 des Sciences de Tunis, Université Tunis El Manar, 2092 Tunis, El Manar, Tunisia

27
28 C. Rumpel

29 Bioemco (UPMC - CNRS - INRA - ENS - UPEC- IRD - AgroParisTech), Centre INRA
30 Versailles-Grignon Bâtiment EGER, 78850 Thiverval-Grignon, France

31
32 Y. le Bissonnais

33 INRA-UMR LISAH (INRA-IRD-Supagro), 2 Place Viala, 34060 Montpellier, France

34
35
36 (✉) **Corresponding author:**

37 Damien Raclot

38 Phone: +33 (0)4 99 61 21 39

39 Fax: +33 (0)4 67 63 26 14

40 e-mail: damien.raclot@ird.fr

43 **Abstract**

1
2 44 Purpose: Approximately 74% of Tunisian agricultural soils are affected by water erosion,
3
4 45 leading to the siltation of numerous man-made reservoirs and therefore a loss of water storage
5
6 46 capacity. The objective of this paper is to propose a methodology for estimating the relative
7
8 47 contributions of gully/channel bank erosion and surface topsoil erosion to the sediment
9
10 48 accumulated in small reservoirs.

11 49 Materials and methods: We tested an approach based on the sediment fingerprinting technique
12
13 50 for sediments collected in a reservoir installed in 1994 at the outlet of a pilot catchment
14
15 51 (Kamech, 2.63 km²). Sampling efforts were concentrated on the soil surface (in both cropland
16
17 52 and grassland), gullies and channel banks. A total of 17 sediment cores were collected along a
18
19 53 longitudinal transect of the Kamech reservoir to investigate the sediment origin throughout
20
21 54 the reservoir. Radionuclides (particularly caesium-137) and nutrients (organic matter, total
22
23 55 phosphorous and total nitrogen) were analysed as potential tracers.

24 56 Results and discussion: The applications of the mixing model with caesium-137 alone or
25
26 57 caesium-137 and total organic carbon provided very similar results: the dominant source of
27
28 58 sediment was surface erosion, which was responsible for 80% of the total erosion within the
29
30 59 Kamech catchment. Additionally, we showed that the analysis of a single composite core
31
32 60 sample provided information on the sediment origin that was consistent with the analysis of
33
34 61 all successive sediment layers observed in the core. We demonstrated the importance of the
35
36 62 core sampling location within the reservoir for obtaining reliable information regarding
37
38 63 sediment sources and the dominant erosion processes.

39 64 Conclusions: The dominance of surface erosion processes indicates that conservation farming
40
41 65 practices are required to mitigate erosion in the Kamech agricultural catchment. Based on the
42
43 66 results from 17 sediment cores, guidelines regarding the number and location of sampling
44
45 67 cores to be collected for fingerprinting purposes are proposed. We showed that the collection
46
47 68 of two cores limited the sediment source apportionment uncertainty due to the core sampling
48
49 69 scheme to less than 10%.

50
51 71 **Keywords** *Catchment • Fingerprinting technique • Reservoir • Gully erosion • Rill and*
52
53 72 *interrill erosion • Source sediment • Core sampling strategy.*

75 **1 Introduction**

76 Soil erosion is a major environmental problem that threatens agricultural sustainability and
77 productivity (EEA 2000; Pimentel et al. 1995). This process disturbs downstream ecosystems
78 by transferring contaminants and nutrients associated with fine-grained sediment from
79 croplands to rivers (Owens et al. 2005). Mediterranean countries are commonly reported to be
80 severely affected by soil erosion due to their climatic instability, poor soil properties, and the
81 occasional use of inappropriate farming practices (e.g., Cantón et al. 2011; Lesschen et al.
82 2008; Mougou et al. 2006). Moreover, climate change projections outline an increase in
83 rainfall intensities, leading to an increased vulnerability of Mediterranean ecosystems. In
84 North African countries, and Tunisia in particular, numerous reservoirs have been constructed
85 in hilly environments in recent decades to provide water for agriculture through surface water
86 mobilisation (Albergel et al. 2005). However, the siltation of these artificial reservoirs due to
87 soil erosion is a major problem, and several existing reservoirs in Tunisia have been
88 completely filled with sediment in less than 10 years (Hentati et al. 2010). Numerous studies
89 have been conducted to quantify erosion rates in Tunisian agricultural regions. Several
90 investigations have used models, such as the Universal Soil Loss Equation (Albergel et al.
91 1998; Ben Cheikha and Gueddari 2008) or the Water Erosion Prediction Project erosion
92 model (Raclot et al. 2006), to estimate or predict the volume of accumulated sediment in
93 catchment reservoirs over several decades. Other studies have focused on the quantification of
94 the gully erosion process using aerial and satellite imagery (Bouchnak et al. 2009; Desprats et
95 al. 2012) or topographic surveys of individual gullies (Collinet and Zante 2005). The majority
96 of these studies implicated gully erosion as the main source of sediment in the Mediterranean
97 region (e.g., de Vente et al. 2006, 2008; Poesen et al. 2003; Roose et al. 2000; Vanmaercke et
98 al. 2012a). Only one recent study, conducted in 28 catchments of Tunisia suggested the
99 dominance of surface (rill/interrill) erosion (Jebari et al. 2010). This result was obtained
100 through an analysis of correspondence between rainfall intensities and dominant erosion
101 processes. However, additional knowledge regarding the sources of sediment (i.e., subsoil
102 exported by gully and channel bank erosion vs. the superficial part of the soil exported by
103 surface erosion) is necessary prior to defining appropriate management strategies to limit
104 erosion at the catchment scale and to increase the reservoir lifetime (Haregeweyn et al. 2012;
105 Vanmaercke et al. 2012b).

106 During the last few decades, fingerprinting techniques have been successfully applied to
107 outline the sources of suspended sediments in rivers or the origin of riverbed, floodplain, and
108 reservoir deposits in several regions of the world (e.g., Collins et al. 2010; Evrard et al. 2011;

109 Walling 2005; Wasson et al. 2010). This technique is often used to identify the contribution of
110 different land use types (Nicholls 2001), lithologies (Russell et al. 2001) or subcatchments
111 (Walling 2005) to the sediment supply at the catchment scale. An overview of the diversity of
112 potential tracing capabilities of various fields of applications with respect to the timescale,
113 spatial scale and grain size is provided by D'Haen et al. (2012). The use of fingerprinting
114 techniques based on radionuclides (^{137}Cs in particular) alone or in combination with other
115 tracers has proven to be effective in discriminating between subsoil and topsoil sources (e.g.,
116 Juracek and Ziegler 2009; Owens 1999; Smith et al. 2012). For example, Zhang and Walling
117 (2005) showed that the magnitude of the ^{137}Cs activity detected within the upper section of a
118 sediment core collected in a lake or a reservoir can provide information on the relative
119 contribution of surface and subsurface sources. Due to the lack of ^{137}Cs fallout during the
120 post-Chernobyl period, ^{137}Cs is an appropriate tracer for investigating the origin of sediment
121 accumulated in a reservoir after 1986.

122 This discrimination between surface and subsurface sources provides important quantitative
123 information on the contribution of various processes that deliver sediment within a catchment.
124 Surface sources can be associated with interrill or rill erosion, whereas subsurface sources are
125 mobilised by gully or channel erosion processes.

126 The presence of fallout radionuclides in significant and measurable quantities in the soils of
127 this region (e.g., Baggoura et al. 1998) enables the use of the fingerprinting technique to
128 quantify the contribution of dominant erosion processes to reservoir deposits and their
129 evolution since the reservoir installation. Organic constituents (e.g., organic carbon) can also
130 be evaluated as potential fingerprints. For example, Albergel et al. (2006) demonstrated that
131 the majority of the organic matter found at two Tunisian dams (El Gouazine and Fidh Ali)
132 originated from upstream soil sources, and this organic matter was not transformed in the
133 recently accumulated sediment (approximately 10 years old in their studies).

134 In addition, although cores collected from natural lakes or artificial reservoirs have been
135 previously analysed using fingerprinting techniques to identify sediment sources (i.e., Foster
136 et al. 2007; He et al. 1996; Zhang et al. 1997), the influence of the number and location of
137 cores collected within this type of deposition area remains to be further investigated.

138 The objectives of this study are as follows: i) to apply the fingerprinting technique to
139 determine the origin of the sediment and assess the contribution of various erosion processes
140 at the scale of a cultivated catchment in Northern Tunisia, and ii) to provide guidelines that
141 define the number and location of cores to be collected within small reservoirs by exploring
142 the vertical and spatial variability of sediment deposits within an artificial reservoir.

143

1 144 **2. Materials and methods**

3 145 **2.1 Study site**

5 146 The Kamech catchment (2.63 km²) is located in a hilly agricultural region of the Northern
7 147 Cape Bon, Tunisia (36.88° N, 10.88° E, Fig. 1). A small reservoir with an initial capacity of
9 148 140,000 m³ was built at the catchment outlet in 1993 and has been in operation since 1994.
11 149 Kamech is an experimental catchment and lacks any erosion mitigation measures. The
12 150 Kamech catchment is a part of the *OMERE* long-term hydro-meteorological observation
14 151 programme (<http://www.umr-lisah.fr/omere>).

16 152 The mean interannual precipitation in the catchment is 650 mm, and the mean interannual
17 153 evapotranspiration ranges up to 1400 mm. Annually ploughed croplands occupy 70% of the
19 154 catchment area and mainly occur on slopes of < 15%. Cereals (wheat, barley, and oats) are the
21 155 dominant crops and are cultivated in rotation with leguminous crops (chickpeas and beans).
23 156 The remaining 30% of the catchment area consists of dwellings, gully and channels features,
25 157 and Mediterranean scrublands. Two main areas of scrubland are present in the catchment. The
27 158 first area corresponds to outcrops of sandstone bars locally covered by very shallow soils. Soil
29 159 export from this area can therefore be neglected. The second scrubland area corresponds to
31 160 non-cultivated steep slopes located in the vicinity of gullies or channels. It covers
33 161 approximately 10% of the catchment area and may be prone to soil export because of
35 162 occasional overgrazing. Therefore, only this second scrubland area was considered as a
37 163 potential sediment source and was sampled in the framework of this study.

38 164 The mean field size is relatively small (0.5 ha), with 40% of the fields having a surface area
40 165 between 0.2 and 0.3 ha. According to the FAO classification (2006), the soil types observed
42 166 within the catchment are Calcic Cambisols (63.5%), Regosols (25.5%), Eutric Regosols
44 167 (9.6%) and Chromic Vertisols (1.4%). Cropland predominantly covers Calcil Cambisols
46 168 whereas gully and channel features predominantly cover Regosols. The majority of these soils
48 169 are characterised by a high clay content (between 25 and 45% when using laser analysis and
50 170 between 30 and 70% when using the pipette sampling method) and a low stoniness (less than
52 171 10%). The bedrock mainly consists of marls and sandstone bars oriented in a southwest to
54 172 northeast direction. The morphology and soil type in the catchment are the result of the
56 173 geological setting such that the soils predominantly vary in a direction perpendicular to the
58 174 sandstone bar outcrops (i.e., the SE-NW direction). Detailed maps showing the topography
60 175 and soil types in Kamech are shown in Raclot and Albergel (2006).

176 The outlet reservoir has an elongated shape with a single major water supply that drains more
177 than 90% of the catchment area. A scour valve for sediment flushing from the reservoir was
178 not constructed, and because overflows are negligible, almost all of the sediment originating
179 from the catchment is trapped within the reservoir. The drainage network has intermittent
180 flow discharge and water in the lake is clear during inter-storm periods.

181 During the period 1994-2008, the estimated mean annual sediment yield based on several lake
182 sedimentation surveys was approximately 15 t.ha⁻¹.year⁻¹; and 11 significant runoff events
183 (runoff > 1 mm) occurred each year on average, among which only two events exceeded 10
184 mm. The accumulated length of the gully and channel features was approximately 20 km in
185 2010 with an estimated annual linear progression of less than 0.2% between 1974 and 2010
186 based on aerial photography.

2.2 Soil and sediment sampling

189 Soil samples representative of the potential sediment source areas were collected in the
190 catchment in September of 2009. All individual samples of source material corresponded to a
191 composite of at least five subsamples collected within an approximate 5 m radius around the
192 sampling point to increase the representativeness of the individual samples. The sampling
193 efforts were concentrated in two areas: (i) the field surface (both croplands and scrublands)
194 and (ii) gullies and channel banks. Areas showing evidence of erosion were given special
195 consideration. For gully and channel sources, sampling was restricted to freshly cut sections
196 in the bottom or the banks (when the features were deeper than 40 cm). The sampling depth
197 was 0-10 cm in croplands and 0-2 cm in scrubland environments. In total, 17 samples
198 representative of the two source types were collected, i.e., between 3 and 4 samples km⁻² for
199 each source. This sampling density is greater than in the majority fingerprinting studies (e.g.,
200 Collins and Walling 2002; Collins et al. 2010; Juracek and Ziegler 2009; Owens and Walling
201 2002; Wasson et al. 2010) and was considered to be sufficient within the context of highly
202 homogeneous soils. In addition, 2 reference samples were collected in areas without soil
203 erosion or deposition, i.e., in flat scrubland areas enclosed within stone walls prior to 1990.
204 Care was taken to ensure that the spatial coverage of all potential sources along the SE-NW
205 direction was representative of the entire range of morphological and pedological conditions
206 observed in the catchment (Fig. 1). At the end, 6 gully/channel samples came from Regosols
207 and 3 from Calcic Cambisols. For the field surface samples, 5 came from cropland on Calcil
208 Cambisols, 1 from cropland on Eutric Regosols and 2 from scrubland on Regosols.

209 Furthermore, 17 sediment cores were collected from a boat during the same period (2009-
210 2010) within the reservoir (Fig. 2a). Each core corresponded to the entire layer of lake
211 sediment at the sampling locations. This completeness was confirmed by the presence of a
212 more compact soil layer at the base of the core; in addition the core depths were consistent
213 with data provided by topographical surveys conducted immediately after the reservoir
214 construction. 13 of these cores (C1 to C13) were located along a downstream-to-upstream
215 transect to capture the influence of the longitudinal core location within the sediment
216 deposition area. Four additional cores were collected to verify that the transversal variability
217 of the sediment core texture and composition was negligible compared to the longitudinal
218 variability. This core sampling strategy was defined based on the concept that reservoir
219 deposits are generally organised according to a longitudinal pattern resulting from both runoff
220 inflow and density current effects (Remini and Remini 2003).

221 A single composite sample was prepared for each core to verify whether it could provide
222 reliable and global information regarding the origin of the entire sediment sequence. The
223 composite sample was prepared by extracting the central part of the core along its entire
224 length. Subsamples corresponding to the sediment deposit sequences of the entire core were
225 also prepared for cores C2 and C9. These cores were first divided into couplets using a
226 complete stratigraphic description as reported by Ambers (2001). The couplets corresponded
227 to single flood events, and the texture and thickness varied depending on the magnitude and
228 the duration of the floods (Ambers 2001). The thicker couplets corresponding to single large
229 flood event were readily identified and individually sampled. In contrast, the thinnest couplets
230 composed of fairly homogeneous fine sediment corresponding to successive low flood events
231 were difficult to isolate and thus regrouped before sampling. As a result, cores C2 and C9
232 were respectively divided into 20 and 11 continuous subsamples that were representative of a
233 large range of flood conditions.

234 235 **2.3 Representativeness of the cores in terms of sediment volume**

236 The volume of sediment accumulated in a reservoir that can be associated with each core can
237 be highly variable as a consequence of the variations in both the sediment thickness and core
238 location patterns within a reservoir.

239 To determine the extent to which each core was representative of the sediment deposits, we
240 employed both initial (1994) and recent (2009) bathymetric surveys using a GIS database.
241 Thiessen polygons were constructed to interpolate between the cores (Fig. 2a). The
242 representativeness of each core in terms of the sediment volume was then derived by

243 calculating the difference between both bathymetric surfaces within each Thiessen polygon
244 and dividing these volumes by the total deposit volume in the Kamech reservoir (Tab. 1).
245 Figure 2b illustrates that sediment accumulation depth is thicker close to the dam than in the
246 upstream part of the reservoir.

2.4 Choice of the fingerprinting properties

249 Two types of fingerprint properties that are commonly considered to be the best tracers to
250 differentiate surface from subsurface soil sources (e.g., Walling 2005) were analysed: (i)
251 radionuclides and (ii) organic constituents.

252 The fallout radionuclide ^{137}Cs is particularly appropriate because it can be considered
253 spatially homogeneous within small catchments, and it is typically characterised by a
254 maximum concentration at the soil surface and a rapid decrease with depth (Wallbrink et al.
255 1999). Consequently, the ^{137}Cs activity in gully or channel-bank material tends to be
256 substantially lower than in surface soils. Moreover, ^{137}Cs has been shown to behave
257 conservatively throughout the sediment generation process (Motha 2002). In the context of
258 sediments trapped in reservoirs built after 1990, ^{137}Cs is likely to be the most reliable fallout
259 radionuclide tracer because caesium fallout has been virtually null in North African countries
260 since the Chernobyl accident in 1986. The burial process has no specific effect on caesium
261 activity, and the direct comparison of its activity between sediment in the reservoir and
262 material sources in the catchment area is feasible.

263 Organic constituents are also often used as tracers although their conservativeness during
264 erosion and sediment delivery processes is less clear than for ^{137}Cs (Collins et al. 1997; Motha
265 et al. 2002; Walling 2005). The magnitude of oxidation of eroded material during transport
266 and after deposition may depend on the composition of particulate organic material (Lal
267 2006), as degradation rates ranging from 0 % (Smith et al. 2001) to 100% (Schlesinger 1995
268 in Lal 2006) have been reported. An analysis of recently accumulated sediments
269 (approximately 10 years old) in two small reservoirs in Tunisia indicated that organic matter
270 was not transformed during this period (Albergel et al 2006). This finding justifies the use of
271 organic carbon as a potential tracer in this region.

2.5 Soil and sediment analysis

274 All soil and sediment samples were first described and then air-dried, hand-disaggregated and
275 sieved through a 2-mm mesh.

276 For the radionuclide measurements of each sample, a small quantity of soil (~80 g) was
277 placed in a counting box. The radionuclide concentrations (^{210}Pb -xs, ^{210}Pb , ^{234}Th , ^{226}Ra , ^{228}Ra ,
278 ^{228}Th , ^{40}K and ^{137}Cs) were determined by gamma-spectrometry using low-background coaxial
279 N- and P-type GeHP detectors (Canberra / Ortec) at the *Laboratoire des Sciences du Climat et*
280 *de l'Environnement* (Gif-sur-Yvette, France). The efficiencies and background levels of the
281 detectors were periodically controlled using internal and International Atomic Energy Agency
282 (IAEA) soil and sediment standards (Evrard et al. 2010). All results were decay-corrected to
283 the day of sampling. The uncertainty associated with radionuclide measurements was less
284 than 5%.

285 The total nitrogen (TN) and total organic carbon (TOC) contents of the soil and sediment
286 were determined at the *Laboratoire Bioemco* (Paris, France) using the HCl-fumigation
287 method and an ANCA-GSL CN analyser (PDZ Europa Ltd., Sandbach, UK) according to the
288 method described by Harris et al. (2001). The analytical uncertainty of these measurements
289 was less than 0.006% (Wilson and Fisher 2011). Stable isotope values of bulk carbon ($\delta^{13}\text{C}$)
290 were also determined using the ANCA-GSL CN analyser coupled to an isotope ratio mass
291 spectrometer (VG Sira 10).

292 The phosphorous contents (P_2O_5) were measured at the *Laboratoire d'Analyses des Sols*
293 *d'Arras* (Arras, France). For the P_2O_5 analyses, samples were dissolved using fluorhydric and
294 perchloric acids (HF - HClO_4) and analysed according to the method described by Ciesielski
295 et al. (1997). Samples of approximately 0.250 g of soil sieved to 250 μm were dosed by
296 plasma emissions in photonic mode (ICP-Atomic Emission Spectroscopy).

297 After the preliminary destruction of organic matter and dispersion of soil particles, the grain-
298 size distribution was determined based on the principle of laser diffraction using a Beckman
299 Coulter LS 13320 particle size analyser at the *Laboratoire Géosciences Montpellier*
300 (Montpellier, France). This device is equipped with an agitator and adjustable ultrasonicator
301 to maintain uniform suspensions, which enables the analysis of particles with diameters
302 between 0.375 and 2000 μm . Typical grain-size fractions (clay < 2 μm , 2 μm < silt < 50 μm
303 and 50 μm < sand < 2 mm) and the specific surface area (SSA, m^2/m^3) were derived from the
304 obtained laser diffraction data.

305 Rock-Eval analyses were performed on six sediment samples corresponding to different depth
306 layers of core C2 at the *Département de Géologie* of the Faculty of Sciences of Tunis
307 (Tunisia). Rock-Eval analyses allow for the detection of the type, thus the origin, of organic
308 carbon (terrestrial source vs. reservoir source). Approximately 100 mg of the sediment core

309 sample was placed in a Rock-Eval 6 analyser, and the results were interpreted based on a
310 Van-Krevelen-type diagram (Espitalié et al. 1985).

311 312 **2.6 Sediment fingerprinting using a mixing model**

313 Differences in the particle size compositions between sediment core and source material were
314 corrected to avoid potential variations that could have affected the fingerprint properties
315 during sediment delivery due to the grain-size selectivity of sediment mobilisation, transport
316 and deposition processes (Collins et al. 1997). He and Walling (1996) tested the particle size
317 effects on the adsorption of ^{137}Cs on soils and sediments and showed that ^{137}Cs content can be
318 closely represented by a power function of the specific surface areas of the samples with
319 exponent values varying between 0.6 and 0.8. In our study, the correction was performed
320 using this power function with an exponent value of 0.7. Each soil source (i.e., surface topsoil
321 and gully/channel bank) was subsequently characterised by its mean concentration/activity
322 and the standard deviation of each of its fingerprint properties.

323 The ability of each potential fingerprinting property to discriminate between the potential soil
324 sources was investigated by conducting a non-parametric Kruskal-Wallis H -test. The null
325 hypothesis stating that measurements of fingerprint properties exhibit no significant
326 differences between source categories was rejected as soon as the H -test statistics reached the
327 fixed critical threshold (typically 0.05).

328 A selection procedure using a stepwise discriminant function analysis (SDFA) was performed
329 to identify the optimal combination of fingerprint properties based on the set of discriminating
330 properties that successfully passed the Kruskal-Wallis H -test. As suggested by Collins and
331 Walling (2002), the minimisation of Wilks' lambda was used as a stepwise selection
332 algorithm to identify the set of parameters that, once combined, were able to correctly and
333 optimally distinguish 100% of the source samples. Wilks' lambda is equal to one when all of
334 the group means are equal. Fingerprinting properties providing a good discrimination of
335 different sources are associated with low lambda values.

336 All tracer properties suspected of non-conservativeness during the erosion process or after
337 deposition were removed from further analysis. ^{210}Pb -xs was also removed because the ^{210}Pb -
338 xs activity in the lake sediments could not be associated with the ^{210}Pb -xs content of the
339 source material alone because the direct fallout to the lake surface with rainfall is continuous.

340 A multivariate Monte Carlo mixing model was then used to account for the actual variability
341 of the fingerprinting properties measured in each source. By assuming a normal distribution
342 for each fingerprinting property and source, a series of 10,000 random positive numbers was

343 generated from these distributions and used to estimate the relative contribution of the
1 344 potential sources in the sediment samples. Such a procedure allowed for the calculation of
2 345 95% confidence intervals. A detailed description of this procedure is provided by Evrard et al.
3 346 (2011).

7 347 Because the conservativeness of organic constituents is not absolutely certain, we chose to
8 348 derive source apportionment based on radionuclides only and used organic constituents as
9 349 complementary tracers in a second step to test whether the addition of those tracers confirmed
10 350 the results of the first step.

14 351

16 352 **3 Results**

18 353 **3.1 Grain-size distribution of the Kamech sources and reservoir deposits**

20 354 Textural information for both the source material and reservoir deposit samples is provided in
21 355 **Table 1**. The grain-size fraction shows very small differences between the two potential
22 356 sources as well as within each source. This result confirms that soils are highly homogeneous
23 357 within the studied catchment.

27 358 In contrast, the textural analysis of all cores revealed a grain-size distribution gradient in the
28 359 reservoir with an increasing proportion of finer sediment fractions in the cores with
29 360 decreasing distance to the dam (**Tab. 1**). Sand particles were only found in the reservoir
30 361 deposits near the stream outlet, whereas the cores collected in the vicinity of the dam were
31 362 exclusively composed of clay and silt particles. This deposition pattern was consistent with
32 363 the fact that sediment tends to become finer grained when being deposited further
33 364 downstream in a reservoir (Morris and Fan 1997).

40 365 Two deposition areas were delineated within the reservoir based on the textural analysis. The
41 366 first deposition area corresponds to the downstream region of the reservoir (e.g., close to the
42 367 dam) and includes cores C1 to C5. This area is characterised by a homogeneous textural
43 368 composition comprising very fine particles and a negligible sand fraction. This area contains
44 369 approximately 75% of the total volume of sediment deposits in the reservoir as deduced from
45 370 the estimated representativeness of the individual cores (C1 to C5, see **Tab. 1**). The second
46 371 deposition area corresponds to the upstream region of the reservoir and includes cores C6 to
47 372 C13. The contribution of the sand fraction in this region varies from 5 to 35% and increases
48 373 with increasing distance to the dam. This less homogeneous area contains 25% of the total
49 374 volume of the sediment deposits.

58 375

376 **3.2. Fingerprinting properties of potential soil sources and sediment core samples**

1 377 The profile variations of the specific surface area and main fingerprint properties (prior to
2 grain-size correction) were determined for cores C2 and C9 as shown in **Figure 3**. A similar
3 378 trend in the concentrations of the different fingerprint properties was observed in each core.
4 379 Overall, the fingerprint properties were less variable in core C2 than in core C9, in which the
5 380 concentrations of both ^{137}Cs and TOC were observed to decrease with depth. The diminution
6 381 of this property decrease for C9 will not be mitigated by a grain-size correction because the
7 382 specific surface area did not show a decreasing trend.
8 383

9 384 Scrubland (restricted to areas showing evidence of erosion) and cropland topsoil samples
10 385 were considered to be one distinct source of surface sediment because they showed similar
11 386 fingerprinting properties values. The qualitative analysis of the fingerprinting properties
12 387 measured in the different soil sources and in the composite sediment core samples collected in
13 388 the reservoir deposits (**Tab. 1**) provided general insight into the origin of the sediment at the
14 389 outlet of the Kamech catchment.

15 390 As expected, ^{137}Cs provided a good level of discrimination between the surface topsoil
16 391 material (with activities systematically greater than 2.2 Bq.kg^{-1}) and the deep soil material
17 392 originating from gullies and channel banks ($< 0.8 \text{ Bq.kg}^{-1}$). In the core samples, the ^{137}Cs
18 393 concentrations ranged between 0.9 and 3.9 Bq.kg^{-1} (**Tab. 1**). A simple analysis using the raw
19 394 data showed that the bulk of the core sediment was supplied by soil surface erosion in the
20 395 cores located near the dam, whereas the contribution of topsoil and subsoil sources was more
21 396 balanced for the upstream cores. TOC analyses corroborated these findings.
22 397

23 398 **3.3 The optimal combination of fingerprinting properties and uncertainty assessment**

24 399 Although five radionuclides passed the Kruskal-Wallis test (**Tab. 2**), four of them were
25 400 rejected due to evidence of non-conservative behaviour, i.e., their concentrations were higher
26 401 in sediment than in both sources. Finally, only ^{137}Cs was retained as a tracer. TOC was also
27 402 identified as a potentially discriminant property, and therefore, its use was tested in
28 403 association with ^{137}Cs in the mixing model (**Tab. 3**) in a second phase of the analysis.
29 404

30 405 The outputs of the Monte Carlo mixing model based on 10,000 simulations consistently
31 406 showed a standard deviation of $\pm 2\%$. therefore, we present only the mean values provided by
32 407 this model in the remaining sections.
33
34
35
36
37
38
39
40
41
42
43
44
45
46
47
48
49
50
51
52
53
54
55
56
57
58
59
60
61
62
63
64
65

3.4 Fingerprinting sediment sources in cores C2 and C9

The sediment sources were derived for both composite core samples, and a sequence of subsamples collected at small vertical intervals within cores C2 and C9. These subsamples corresponded to the succession of one or more storm events since the creation of the artificial reservoir. The mixing models using ^{137}Cs only or ^{137}Cs in association with TOC showed very similar results (Fig. 4). Differences in the sediment source apportionment were not significant and were consistently less than 2% for all subsamples, i.e., on the same order of magnitude as the precision of the mean value calculated by the Monte-Carlo procedure.

The results showed that the origin of the sediment estimated from the composite sample was consistent with the origin estimated for the entire sequence of subsamples. Therefore, the composite sample was shown to provide reliable information, which remains valid for the entire core, on the origin of sediment and associated erosion processes.

The subsample analysis of the sequence of sediment deposits within the cores (e.g., 20 sequences for 15 years in core C2) showed that the temporal variability in the sediment sources was low in each core. These results confirm the relevance of analysing a single composite sample for each core to obtain global information regarding the dominant erosion sources and processes that occurred within the catchment over several decades. The mixing model results showed a clear predominance of the surface topsoil source for core C2 (> 80%), whereas sediment in core C9 was supplied by a more even combination of surface and subsurface/bank sources.

3.5 Fingerprinting sediment sources in the 13 composite core samples

Source sediment apportionments for the 13 composite core samples taken along the AA' transect were also evaluated using either ^{137}Cs only or ^{137}Cs in association with TOC as fingerprint properties. The differences between both types of results were again < 2% for all composite core samples with the exception of C13, in which difference was 6% (Fig. 5).

These results demonstrate the major effect of the location of the core sampling site within the reservoir deposit area. Similar results were obtained for cores C1 to C5 with a clear predominance of the surface topsoil contribution (between 80 and 100%). For cores C6 to C13, which were more distant from the dam, the mixing model shows that a larger proportion of sediment was supplied by the gully-channel bank source (between 30 and 75%). The variability of sediment sources is thus higher in the upstream area of the reservoir deposits than in the area closer to the dam, with a trend towards a higher gully-channel bank contribution with increasing distance from the dam.

442 A global fingerprinting result for all the sediment deposits was established by calculating a
1 443 weighted average of the source contribution derived from the 13 composite core samples with
2 444 the representative sediment volume of each core as weighted value (see **Tab 1**). Based on this
3 445 calculation, we obtained a global picture of the sources delivering sediment to the reservoir at
4 446 the outlet of the Kamech catchment. This global value for the reservoir clearly demonstrated
5 447 that the surface topsoil is the dominant source of sediment within the Kamech catchment and
6 448 supplied 80% of the sediment to the outlet reservoir.
7 449

14 450 **4 Discussion**

16 451 **4.1 Spatial variability and core sampling optimisation**

18 452 The spatial variability of the sediment texture within the reservoir trends in an upstream-
19 453 downstream direction (**Tab. 1**). This result is in agreement with transport sedimentation
20 454 selection processes, i.e., the sedimentation of suspended fine particles occurs by vertical
21 455 silting in the quiescent downstream region of the reservoir. In contrast, the upstream part of
22 456 the reservoir is characterised by a higher velocity, and the runoff inflow and deposition
23 457 mainly affects the coarser grain-size particles by both vertical silting and bedload processes.

24 458 The ^{137}Cs and TOC contents were also affected by the contrasting sedimentation processes in
25 459 these two sedimentation areas (**Tab. 1**). This result is consistent with a study conducted on
26 460 sediments of the Yesa reservoir in the Spanish Pyrenees showing that the distribution of
27 461 radionuclides along a transect of bottom reservoir sediments from the delta to the dam was
28 462 influenced by the sediment dynamics and flood events (Navas et al. 2011).

29 463 More surprisingly, the results of the mixing model (**Figure 5**) for the different cores proved to
30 464 be dependent on their location in the reservoir . However, it is unlikely that the source of the
31 465 deposited sediment changes across the reservoir, as both potential sources are not
32 466 characterised by clearly distinct particle size distributions. The most convincing explanation is
33 467 that the standard particle size correction factor based on the SSA derived from laser
34 468 measurements failed to fully address this problem. Preliminary investigations on the effect of
35 469 the exponent value on the grain-size correction function were conducted by testing values in
36 470 the range [0.5; 1]. The global fingerprinting result for the entire reservoir was only slightly
37 471 impacted by the exponent value, as the contribution of the surface source varied only from
38 472 78.9 to 83.9%. Similarly, **Figure 6** shows that the fingerprinting results for the cores located in
39 473 the downstream part of the reservoir were not significantly affected. In contrast, cores
40 474 collected in the upstream part of the reservoir were significantly affected. An exponent value
41 475 of 1 provided slightly less pronounced differences between the downstream and upstream
42
43
44
45
46
47
48
49
50
51
52
53
54
55
56
57
58
59
60
61
62
63
64
65

476 areas, although these differences remained excessively high for the correction to be consider
1 477 satisfactory. The choice of the exponent value was clearly not the main reason for this failure,
2
3 478 and the function itself should be questioned. SSA may fail because the assumption of
4
5 479 spherical particles is clearly not systematically valid, and adsorption behaviour may be highly
6
7 480 dependent on the nature of the minerals — especially in the finer fraction — and not only on
8
9 481 their grain size. Additional research on the grain-size correction factor is required to improve
10
11 482 the reliability of the fingerprinting technique using this type of tracers.

12
13 483 Zonation induced by transport sedimentation processes finally proved to be a key element for
14
15 484 the interpretation of mixing model results and for establishing a core sampling strategy when
16
17 485 using the standard particle size correction factor.

18 486 A comparison of the mixing model estimation derived from a weighted average of the 13
19
20 487 composite cores (reference value) and the results obtained for each core provides a
21
22 488 mechanism for evaluating the relevance of the reservoir coring strategy and deriving
23
24 489 important guidelines (location and number) for future core sampling optimisation. We
25
26 490 calculated the absolute errors in the source apportionment for the following three core
27
28 491 sampling strategies (Tab. 4): sampling of a single core in the downstream reservoir area,
29
30 492 sampling of a single core in the upstream reservoir area, and sampling of two cores (one in
31
32 493 each area).

33 494 This calculation shows that the sampling of a single core in the downstream reservoir area
34
35 495 will lead to a mean absolute error of approximately 7.5% (in this case, generating an
36
37 496 overestimation of the surface topsoil contribution), whereas the sampling of a single core in
38
39 497 the upstream reservoir area will lead to a larger error of approximately 25% (i.e., an
40
41 498 underestimation of the surface contribution) (see Tab. 4). For the core sampling strategy
42
43 499 based on two cores — one in the downstream reservoir area and the other in the upstream
44
45 500 reservoir area — we applied a weight equal to 75% for the core collected in the downstream
46
47 501 area and a weight of 25% for the core collected in the upstream area to account for the
48
49 502 volumetric representation of both deposition areas. This strategy provided a means of
50
51 503 decreasing the absolute mean error to less than 4% and the maximum error to less than 10%
52
53 504 in the studied catchment.

54
55 505 Based on this assessment, an optimised core sampling strategy for the Kamech reservoir
56
57 506 deposits can be based on the collection of a single core in the downstream reservoir deposit
58
59 507 area if a maximal source estimation error of 15% can be accepted. Otherwise, a maximal
60
61 508 source estimation error of 10% can be obtained if we conduct a dual-core sampling strategy.
62
63
64
65

509 We believe that such a result may be generalised to other small reservoirs in Tunisia even if
510 the 75%-25% apportionment between fine sediment in the downstream part of the reservoir
511 and coarse deposits in the upstream part of the reservoir found in Kamech remains to be
512 verified in other reservoirs characterised by a different shape, for example. We also believe
513 that a core sampling scheme that combines the collection of cores in both upstream and
514 downstream parts of the deposits will provide small errors in the results, independent of the
515 number of potential sediment sources. In the case of reservoirs characterised by multiple
516 tributaries, we suggest that the analysis of a core in the downstream part of the reservoir be
517 combined with that of one core for each upstream area influenced by each tributary.
518 Finally, we also determined the relevance of analysing a single composite sample for each
519 core to obtain synthetic information on the main erosion sources and processes that occurred
520 within the catchment over several decades. This result has important practical and financial
521 implications for the future application of this method in a similar context (e.g., sediment
522 deposits in small-catchment reservoirs built during the 1990s in Maghreb) because it
523 simplifies the core sampling process due to a lower diameter requirement and permits cost-
524 savings, as only one sample must to be analysed for each core.

4.2 On the ability to use TOC as tracer in recent North African reservoirs

527 The use of multiple tracers in a mixing model allows for more reliable source apportionment
528 than the use of only one tracer (Martinez-Carreras et al. 2008; Small et al. 2001; Walling et al.
529 1993). In this study, TOC was tested as a tracer in addition to fallout radionuclides. The
530 combined use of ^{137}Cs and TOC provided results similar to those obtained using ^{137}Cs alone.
531 This ability of TOC to be used as an additional tracer in this study can be explained by the
532 specific context of recently built North African reservoirs (less than 20 years old). First, the
533 autochthonous source of organic constituents was found to be negligible in a series of more
534 than 20 modern reservoirs where very low values of dissolved P and N have been measured
535 (Rahaingomanana 1998). Recent complementary analyses confirmed that the Kamech
536 reservoir is characterised by low levels of dissolved N and P. The terrestrial origin of TOC
537 was also verified for the Kamech reservoir using Rock-Eval analysis conducted on upper,
538 middle and bottom subsamples of core C2 (Fig. 7). This result was also corroborated by $\delta^{13}\text{C}$
539 measurements conducted for all the C2 and C9 subsamples and the surface topsoil samples, as
540 all of the values of $\delta^{13}\text{C}$ ranged from -27 to -26‰ which is indicative of the contribution of C_3
541 photosynthetic pathway plants (i.e., wheat crop residues in this case).

542 Moreover, terrestrial organic residues probably did not experience major changes via bacterial
1 543 alteration during their settling and incorporation into the sediment because terrestrial higher
2 544 plant debris had already been submitted to strong biotic as well as abiotic degradation under
3 545 oxic conditions in soils (Vandenbroucke and Largeau 2007). In our study area, degradation
4 546 during mobilisation and transport is also limited due to the very short sediment transport
5 547 distances within the 2.63 km² Kamech catchment.

10 548 Degradation during the sediment storage period was also proved to be limited as no clear
11 549 downcore decrease in the evolution of TOC was observed within the C2 core. This result is
12 550 consistent with other observations from oligotrophic lacustrine environments such as the Lac
13 551 du Bouchet (France), for which Patience et al. (1995) reported a first-order kinetics of TOC
14 552 degradation of $2.2 \cdot 10^{-3} \text{ y}^{-1}$. A similar degradation rate within a 15-years-old reservoir such as
15 553 Kamech would generate a relative decrease in the TOC concentration of less than 2.5%. This
16 554 low degradation rate is likely not valid for upstream deposits because C9 core showed a
17 555 downcore trend of decreasing TOC values.

25 556

27 557 **4.3 Erosion processes and sediment source hierarchy at the catchment scale**

28 558 The determination of the sediment sources in the core samples collected in the Kamech
29 559 catchment reservoir (Cape Bon, Tunisia) using a fingerprinting method showed that the
30 560 surface topsoil delivered approximately 80% of the sediment to the Kamech catchment outlet
31 561 over a period of 15 years. This result implies that surface erosion processes, including rill and
32 562 interrill erosion, are the dominant processes at the catchment scale. This result is consistent
33 563 with the rather low annual gully length progression observed in the catchment. It is also in
34 564 agreement with the results obtained by Jebari et al. (2010), who calculated that interrill
35 565 processes produced 83% of the erosion within the Kamech catchment based on a rainfall
36 566 erosivity analysis. However, the results present here differ from the conclusions of several
37 567 other erosion studies conducted in the Mediterranean region that indicate a predominance of
38 568 gully erosion. One explanation for this difference may be that the low rates of sheet and rill
39 569 erosion and the relatively large importance of gully erosion in the Mediterranean region have
40 570 often been attributed to the high extent of stoniness and shallow depth of many Mediterranean
41 571 soils (e.g. Poesen and Hooke 1997), which is not the case in the studied catchment.

54 572 The potential surface sediment sources in Kamech catchment include both cropland and
55 573 scrubland except in the sandstone bar outcrops. However, there are several indications that
56 574 topsoil in the cropland area is by far the most important sediment source. First, the scrubland
57 575 area covers only 10% of the catchment surface, whereas the cropland area represents 70% of

576 the catchment area. Second, all of the cropland areas are likely to provide sediment, whereas
577 only very limited scrubland areas suffering from over-grazing must be considered as sediment
578 sources. Finally, the continuous multi-scale monitoring of erosion over a 4-year period
579 showed that the sediment yield measured at the outlet of a 0.16 km² subcatchment in Kamech
580 reached 22 t.ha⁻¹.year⁻¹, 75% of this material was supplied by cropland and 25% by gully
581 banks and bottoms, and the contribution of scrubland source remained negligible (Sauvadet et
582 al., 2012). These measurements strongly supported the results derived in this study from the
583 mixing models.

584 We also observed a low variability in ¹³⁷Cs and TOC in the different couplets of core C2 and
585 C9, although those couplets could be related to a large range of flood event conditions. This
586 result suggests that flood conditions over the 15-year existence of the reservoir did not
587 strongly affect the sediment origin in the Kamech catchment. I.e., no exceptional flood event
588 during which gully/channel erosion processes would have become a predominant source
589 could be identified in the Kamech catchment.

591 **5 Conclusions**

592 This study demonstrated the viability of the fingerprinting method for tracing sediment
593 sources in recent (i.e. post-Chernobyl) small artificial reservoir deposits using both ¹³⁷Cs and
594 TOC. Therefore, this method can be used to quantify the relative importance of hillslope
595 surfaces versus gully-channel bank erosion processes in North African environments. Several
596 other radionuclides or nutrients were also tested as potential tracers of sediment sources but
597 they did not deliver good results. The explanation is either their non conservativeness during
598 the transport and deposition processes or their poor efficiency in discriminating between
599 subsoil and topsoil sources. The determination of the sediment origin in the core samples
600 collected in the Kamech catchment reservoir (Cape Bon, Tunisia) revealed surface soil
601 erosion as the dominant source of deposited material. These results differ from the
602 conclusions of most erosion studies conducted in the Mediterranean region that show a
603 predominance of gully erosion. This finding has important management implications because
604 the implementation of conservation farming practices would be more efficient than gully
605 treatment for erosion mitigation in agricultural catchments similar to the Kamech study site.
606 The predominance of one source of erosion in a catchment may, however, depend on specific
607 conditions that are not yet fully understood. The strategy applied here of collecting a series of
608 sediment cores along a longitudinal transect within the outlet reservoir provided a means of
609 investigating the potential representativeness of a single sediment core collected within the

610 reservoir. Practical guidelines for conducting core sampling in small reservoirs were derived
1 611 as follows: i) a composite core sample provides a good representation of the entire core length
2 612 according to the homogeneity observed in the two sediment cores that were analysed in
3 613 greater detail; ii) a two-core sampling strategy allows for the evaluation of source
4 614 contributions with an error of less than 10% for the studied catchment. We also suggest
5 615 adjusting the number of cores as a function of the number of main tributaries that supply
6 616 material to the studied reservoir. This strategy developed and tested in the Kamech catchment
7 617 can now be applied to the numerous existing reservoirs located in the Tunisian Ridge and
8 618 Cape Bon areas. This region is affected by severe erosion, and it is crucial to determine the
9 619 relative contributions of surface erosion and gully erosion in various contrasting catchments
10 620 to address the controversial issue of outlining the dominant erosion process that deliver the
11 621 bulk of sediment in this type of Mediterranean environment. This determination of the
12 622 dominant erosion process should allow to propose management guidelines that are adapted for
13 623 each catchment to control erosion.
14
15
16
17
18
19
20
21
22
23
24

25 624

27 625 **Acknowledgements** This study was financially supported by the IRD-DSF, SCAC of French
28 626 embassy and a CNRS/DGRS exchange agreement (No. 24443) between France and Tunisia.
29 627 This study was performed within the framework of the OMERE Observatory funded by
30 628 INRA and IRD. We thank three anonymous reviewers for their insightful comments, which
31 629 greatly improved this manuscript.
32
33
34
35

36 630

38 631 **References**

40 632 Albergel J, Boufaroua M, Pepin Y (1998) Bilan de l'érosion sur les petits bassins versants des
41 633 lacs collinaires en climat semi-aride Tunisien. Bulletin Réseau Erosion 18:67-75
42 634 Albergel J, Collinet J, Pépin Y, Zante P, Nasri S, Boufaroua M, Droubi A, Merzouk A (2005)
43 635 The sediment budgets of hill reservoirs in small catchments in North Africa and the
44 636 middle East. Sediment Budgets 1, Book Series: IAHS Publ 291:323-331
45 637 Albergel J, Mansouri T, Zante P, Ben Mamou A, Abdeljaoued S (2006) Organic carbon in the
46 638 sediments of hill dams in a semiarid Mediterranean area. In: Roose E, Lal R, Feller C,
47 639 Barthès B, Stewart BA (eds) Soil erosion and carbon dynamics. Taylor et Francis, Boca
48 640 Raton, pp 289-299
49 641 Ambers RKR (2001) Using the sediment record of western Oregon flood-control reservoir to
50 642 assess the influence of storm history and logging on sediment yield. Journal of hydrology
51 643 244:181-200
52
53
54
55
56
57
58
59
60
61
62
63
64
65

- 644 Baggoura B, Nouredine A, Benkrid M (1998) Level of natural and artificial radioactivity in
1 645 Algeria. *Appl Radiat Isotopes* 49(7): 867-873
- 3 646 Ben Cheikha L, Gueddari M (2008) Le bassin versant de Jannet (Tunisie): évaluation des
4 647 risques d'érosion hydrique. M@ppemonde 90 (2008.2).
6 648 <http://mappemonde.mgm.fr/num18/articles/art08202.pdf>
- 8 649 Bouchnak, H, Felfoul MS, Boussema MR, Snane MH (2009) Slope and rainfall effects on the
10 650 volume of sediment yield by gully erosion in the Souar lithologic (Tunisia). *Catena*
11 651 78(2):170-177
- 13 652 Cantón Y, Solé-Benet A, de Vente J, Boix-Fayos C, Calvo-Cases A, Asensio C,
14 653 Puigdefábregas J (2011) A review of runoff generation and soil erosion across scales in
15 654 semiarid south-eastern Spain. *J Arid Environ* 75(12):1254-1261
- 17 655 Ciesielski H, Proix N, Sterckeman T (1997) Détermination des incertitudes liées à une
18 656 méthode de mise en solution des sols et des sédiments par étude inter-laboratoire.
19 657 *Analysis* 25:188-192
- 21 658 Collinet J, Zante P (2005) Analyse du ravinement de bassins versants à retenues collinaires
22 659 sur sols à fortes dynamiques structurales (Tunisie). *Géomorphologie 1: relief, processus,*
23 660 *environnement* 1:61-74
- 25 661 Collins AL, Walling DE (2002) Selecting fingerprint properties for discriminating potential
26 662 suspended sediment sources in river basins. *J Hydrol* 261:218-244
- 28 663 Collins AL, Walling DE, Leeks GJL (1997) Source type ascription for fluvial suspended
29 664 sediment based on a quantitative composite fingerprinting technique. *Catena* 29:1-27
- 31 665 Collins AL, Walling DE, Webb L, King P (2010) Apportioning catchment scale sediment
32 666 sources using a modified composite fingerprinting technique incorporating property
33 667 weightings and prior information. *Geoderma* 155:249-261
- 35 668 Desprats JF, Raclot D, Rousseau M, Cerdan O, Garcin M, Le Bissonnais Y, Ben Slimane A,
36 669 Fouche J, Monfort-Climent D (2012) Satellite imagery mapping of linear erosion
37 670 features. *Land Degradation & Development*. doi: 10.1002/ldr.1094
- 39 671 D'Haen K, Verstraeten G, Degryse P (2012) Fingerprinting historical fluvial sediment fluxes.
40 672 *Progress in Physical Geography* 36:154-186
- 42 673 de Vente J, Poesen J, Bazzofi P, Van Rompaey A, Verstaeten G (2006) Predicting catchment
43 674 sediment yield in Mediterranean environments: the importance of sediment sources and
44 675 connectivity in Italian drainage basins. *Earth Surf Proc Land* 31:1017-1034

676 de Vente J, Poesen J, Verstraeten G, Van Rompaey A, Govers G (2008) Spatially distributed
1 677 modelling of soil erosion and sediment yield at regional scales in Spain. *Global and*
2 678 *Planetary Change* 60:393-415
3
4
5 679 EEA (2000) *Down to earth: Soil degradation and sustainable development in Europe, A*
6 680 *challenge for the 21st century*. Environmental issues series 16. Office for Official
7 681 Publications of the European Communities, Luxembourg
8
9
10 682 Espitalié J, Deroo G, Marquis F (1985) La pyrolyse Rock-Eval et ses applications. *Revue de*
11 683 *l'Institut Francais du Petrole*, Part I 40:563–578, Part II 40:755–784; Part III 41:73–89
12
13
14 684 Evrard O, Némery J, Gratiot N, Duvert C, Ayrault S, Lefèvre I, Poulenard J, Prat C, Bonté P,
15 685 Esteves M (2010) Sediment dynamics during the rainy season in tropical highland
16 686 catchments of central Mexico using fallout radionuclides. *Geomorphology* 124:42–54
17
18
19 687 Evrard O, Navratil O, Ayrault S, Ahmadi M, Némery J, Legout C, Lefèvre I, Poirel A, Bonté
20 688 P, Esteves M (2011) Combining suspended sediment monitoring and fingerprinting to
21 689 determine the spatial origin of fine sediment in a mountainous river catchment. *Earth*
22 690 *Surf Proc Land* 36:1072–1089
23
24
25 691 Foster IDL, Boardman J, Keay-Brighth J (2007) Sediment tracing and environmental history
26 692 for two small catchments, Karoo Uplands, South Africa. *Geomorphology* 90:126-143
27
28
29 693 Haregeweyn N, Melesse B, Tsunekawa A, Tsubo M, Mesheshe D, Babullo Balana B (2012)
30 694 Reservoir sedimentation and its mitigating strategies: a case study of Angered reservoir
31 695 (NW Ethiopia). *Journal of Soils and Sediments* 12:291-305
32
33
34 696 Harris D, Horwath WR, Kessel CV (2001) Acid fumigation of soils to remove carbonates
35 697 prior to total organic carbon or carbon-13 isotopic analysis. *Soil Sci Soc Am J* 65:1853–
36 698 1856
37
38
39 699 He Q, Walling DE (1996) Interpreting particle size effects in the adsorption of ¹³⁷Cs and
40 700 unsupported ²¹⁰Pb by mineral soils and sediments. *J Environ Radioactivity* 30:117-137
41
42
43 701 He Q, Walling DE, Owens PN (1996) Interpreting the ¹³⁷Cs profiles observed in several
44 702 small lakes and reservoirs in southern England. *Chem Geol* 129:115-131.
45
46
47 703 Hentati A, Kawamura A, Amaguchi H, Iseri Y (2010) Evaluation of sedimentation
48 704 vulnerability at small hillside reservoirs in the semi-arid region of Tunisia using the Self-
49 705 Organizing Map. *Geomorphology* 122:56-64
50
51
52 706 Jebari S, Berndtsson R, Bahri A, Boufaroua M (2010) Spatial soil loss risk and reservoir
53 707 siltation in semi-arid Tunisia. *Hydrolog Sci J* 55(1):121-137
54
55
56 708 Juracek KE, Ziegler AC (2009) Estimation of sediment sources using selected chemical
57 709 tracers in the Perry lake basin, Kansas, USA. *Int J Sediment Res* 24(1):108-125
58
59
60
61
62
63
64
65

- 710 Lal R (2006) Influence of soil erosion on carbon dynamics in the World. In: Roose E, Lal R,
1 711 Feller C, Barthès B, Stewart BA (eds) Soil erosion and carbon dynamics. Taylor et
2 Francis, Boca Raton, pp 23-35
3 712
4
5 713 Lesschen JP, Cammeraat LH, Nieman T (2008) Erosion and terrace failure due to agricultural
6 land abandonment in a semi-arid environment. *Earth Sur Proc Land* 33(10):1574-1584
7 714
8
9 715 Martinez-Carreras N, Gallart F, Iffly JF, Pfister L, Walling DE, Krein A (2008) Uncertainty
10 assessment in suspended sediment fingerprinting based on tracer mixing models: a case
11 716 study from Luxembourg. In: Schmidt J, Cochrane T, Phillips C, Elliot S, Davies T,
12 717 Basher L (eds) Sediment dynamics in changing environments. IAHS Publ 325,
13 Wallingford, pp 94–105
14 718
15
16 719
17
18 720 Mougou R, Mansour M, Vacher J, Cellier P (2006) La valorisation agricole de l'eau des lacs
19 collinaires: cas du lac collinaire Kamech (Tunisie). *Sécheresse* 17(3):385-90
20 721
21
22 722 Morris GL, Fan J (1997) Reservoir Sedimentation Handbook. McGraw-Hill, New York
23
24 723 Motha JA, Wallbrink PJ, Hairsine PB, Grayson RB (2002) Tracer properties of eroded
25 sediment and source material. *Hydrol Process* 16:1983–2000
26 724
27 725 Navas A, Valero-Garcés B, Gaspar L, Palazón L (2011) Radionuclides and stable elements in
28 the sediments of the Yesa Reservoir, Central Spanish Pyrenees. *Journal of Soils and*
29 726 *Sediments* 11:1082-1098
30
31 727
32
33 728 Nicholls DJ (2001) The source and behaviour of fine sediment deposits in the River Torridge
34 Devon and their implications for salmon spawning. Unpublished PhD thesis, University
35 729 of Exeter
36 730
37
38 731 Owens PN, Walling DE (2002) Changes in sediment sources and floodplain deposition rates
39 in the catchment of the River Tweed, Scotland, over the last 100 years: The impact of
40 732 climate and land use change. *Earth Surf Proc Land* 27:403-423
41
42 733
43 734 Owens PN, Walling DE, Leeks GJL (1999) Use of floodplain sediment cores to investigate
45 recent historical changes in overbank sedimentation rates and sediment sources in the
46 735 catchment of the River Ouse, Yorkshire, UK. *Catena* 36:21-47
47
48
49 737 Owens PN, Batalla RJ, Collins AJ, Gomez B, Hicks DM, Horowitz AJ, Kondolf GM, Marden
50 M, Page MJ, Peacock DH, Peticrew EL, Salomons W, Trustrum NA (2005) Fine-
51 738 grained sediment in river systems: environmental significance and management issues.
52 739 *River Res Appl* 21:693-717
53
54 740
55
56 741 Patience AJ, Lallier-Vergès E, Sifeddine A, Albéric P, Guillet B (1995) Organic fluxes and
57 early diagenesis in the lacustrine environment: the superficial sediments of the Lac du
58 742 Bouchet (Haute Loire, France). In: Lallier-Vergès E, Tribovillard N, Bertrand P (eds)
59
60 743

- 744 Organic Matter Accumulation: The Organic Cyclicities of the Kimmeridge Clay
1 745 Formation (Yorkshire, G.B.) and the Recent Maar Sediments (Lac du Bouchet). Lecture
2 Notes in Earth Sciences 57. Springer-Verlag, Heidelberg, pp 145–156
3 746
4
5 747 Pimentel D, Harvey C, Resosudarmo P, Sinclair K, Kurz D, McNair M, Crist S, Shpritz L,
6 Fitton L, Saffouri R, Blair R (1995) Environmental and economic costs of soil erosion
7 748 and conservation benefits. *Science*, new series 267(5201):1117–1123
8 749
9
10 750 Poesen J, Hooke J (1997) Erosion, flooding and channel management in Mediterranean
11 environments of southern Europe. *Progress in Physical Geography* 21:157-199
12 751
13
14 752 Poesen J, Nachtergaele J, Verstraeten G, Valentin C (2003) Gully erosion and environmental
15 change: importance and research needs. *Catena* 50(2/4):91-133
16 753
17
18 754 Raclot D, Albergel J (2006) Runoff and water erosion modelling using WEPP on a
19 Mediterranean cultivated catchment. *Phys Chem Earth* 31(17):1038-1047
20 755
21
22 756 Rahaingomanana N (1998) Caractérisation géochimique des lacs collinaires de la Tunisie
23 semi-aride et régulation géochimique du phosphore. PhD thesis, Univ. Montpellier I
24 757
25 758 Remini W, Remini B (2003) La sédimentation dans les barrages de l’Afrique du nord.
26 *Larhyss Journal* 2: 45-54
27 759
28
29 760 Roose E, Chebbani R, Bourougaa L (2000) Ravinement en Algérie, facteurs de contrôle,
30 quantification et réhabilitation. *Science et changements planétaires/ Sécheresse*
31 761 11(4):317-326
32 762
33
34 763 Russell MA, Walling DE, Hodgkinson RA (2001) Suspended sediment sources in two small
35 lowland agricultural catchments in the UK. *J Hydrol* 252:1-24
36 764
37
38 765 Sauvadet M, Raclot D, Ben Slimane A, Le Bissonnais Y (2012) Déterminisme du
39 ruissellement et de l’érosion hydrique de la parcelle au versant en milieu méditerranéen
40 766 marneux. *Revue Marocaine des Sciences Agronomiques Vétérinaires* 1:41-46.
41 767 http://www.agrimaroc.org/index.php/Actes_IAVH2/article/view/282/248.
42 768
43
44 769 Schlesinger WH (1995) Soil respiration and changes in soil carbon stocks. In: Woodwell GM,
45 Mackenzie FT (eds) *Biotic Feedbacks in the Global Climate System*. Oxford University
46 Press, Oxford, pp 159-168
47 770
48
49 771 Small IF, Rowan JS, Franks SW (2002) Quantitative sediment fingerprinting using a Bayesian
50 uncertainty estimation framework. In: Dyer FJ, Thoms MC, and Olley JM (eds)
51 772 *Structure, Function and Management Implications of Fluvial Sedimentary Systems*.
52 IAHS Publ 276, Wallingford, pp 443-450
53 773
54 774
55
56 775
57
58
59
60
61
62
63
64
65

- 776 Smith SV, Renwick WH, Buddemeier RW, Crossland CJ (2001) Budgets of soil erosion and
1 777 deposition for sediments and sedimentary organic carbon across the conterminous United
2 778 States. *Global Biogeochem Cy* 15:697–707
3
4
5 779 Smith HG, Sheridan GJ, Nyman P, Child DP, Lane PNJ, Hotchkis MAC, Jacobsen GE (2012)
6
7 780 Quantifying sources of fine sediment supplied to post-fire debris flows using fallout
8
9 781 radionuclide tracers. *Geomorphology* 139-140:403-415
10
11 782 Vandembroucke M, Largeau C (2007) Kerogen origin, evolution and structure. *Organic*
12 783 *Geochemistry* 38:719-833
13
14 784 Vanmaercke M, Poesen J, Verstraeten G, Maetens W, de Vente J (2012a) Sediment yield as a
15
16 785 desertification risk indicator. *Science of the Total Environment* 409:1715-1725
17
18 786 Vanmaercke M, Maetens W, Poesen J, Jankauskas B, Jankauskiene G, Verstraeten G, de
19
20 787 Vente J (2012b) A comparison of measured catchment sediment yields with measured
21
22 788 and predicted hillslope erosion rates in Europe. *J Soils Sediments* 12:586-602
23
24 789 Wallbrink PJ, Murray AS, Olley JM (1999) Relating suspended sediment to its original soil
25 790 depth using fallout radionuclides. *Soil Sci Soc Am J* 63:369–378
26
27 791 Walling DE (2005) Tracing suspended sediment sources in catchments and river systems. *Sci*
28
29 792 *Total Environ* 344:159-184
30
31 793 Walling DE, Woodward JC, Nicholas AP (1993) A multi-parameter approach to fingerprint
32
33 794 suspended-sediment sources. In: Peters NE, Hoehn E, Leibundgut C., Tase N, Walling
34 795 DE (eds) *Tracers in hydrology*. IAHS Publ 215, Wallingford, pp 329-338
35
36 796 Wasson RJ, Furlonger L, Parry D, Pietsch T, Valentine E, Williams D (2010) Sediment
37
38 797 sources and channel dynamics, Daly River, Northern Australia. *Geomorphology*
39
40 798 114:161-174
41
42 799 Wilson JP, Fischer WW (2011) Geochemical Support for a Climbing Habit within the
43
44 800 Paleozoic Seed Fern Genus *Medullosa*. *Int J Plant Sci* 172(4):586–598
45
46 801 Zhang X, Walling DE (2005) Landscape and Watershed Processes: Characterizing Land
47 802 Surface Erosion from Cesium-137 Profiles in Lake and Reservoir Sediments. *J Environ*
48
49 803 *Qual* 34:514-52
50
51 804 Zhang X, Walling DE, Quine TA, Wen A (1997) Use of reservoir deposits and caesium-137
52
53 805 measurements to investigate the erosional response of a small drainage basin in the rolling
54
55 806 loess plateau region of China. *Land Degrad Dev* 8:1-96
56
57 807
58 808
59
60
61
62
63
64
65

809 **Figure legends**

1 810

2
3 811 **Fig. 1** Location and aerial view of the Kamech catchment. The source sampling sites are shown.

4 812

5
6 813 **Fig. 2** Core sampling locations within the Kamech reservoir and Thiessen polygons outlines based on the cores
7 814 C1 to C13 (a); and the AA' longitudinal section view of the sediment deposit depths with the locations of the 13
8
9 815 associated cores (b).

10 816

11
12 817 **Fig. 3** Downcore variations in the specific surface area and selected fingerprint properties for cores C2 and core
13 818 C9

14
15 819

16 820 **Fig. 4** Surface topsoil apportionment derived using the mixing model — either with the combination of caesium
17
18 821 and carbon or with caesium only — for the sequences of the two cores C2 and C9 collected in the Kamech
19 822 reservoir. The value derived from the composite core sample is also presented. Note that the complementary
20
21 823 contribution of surface topsoil erosion is provided by gully or channel-bank erosion.

22 824

23
24 825 **Fig. 5** Surface topsoil apportionment in the Kamech catchment according to the core location along the AA'
25
26 826 transect. The weighted average for the 13 composite core samples is also represented. Note that the
27 827 complementary contribution of surface topsoil erosion is provided by gully or channel-bank erosion.

28 828

29 829

30
31 830 **Fig. 6** Sensitivity of the surface source derived from fingerprinting results to the exponent value in the grain-size
32
33 831 correction function. The result without any grain-size correction is also depicted.

34 832

35
36 833 **Fig. 7** Kerogen type and evolution paths (arrows) in the van Krevelen diagram of HI vs. OI. Kerogen types I, II,
37
38 834 and III correspond to waxy organic matter, algal organic matter and vascular plant organic matter, respectively.

39 835

40
41
42 836

43

44

45

46

47

48

49

50

51

52

53

54

55

56

57

58

59

60

61

62

63

64

65

1
2
3
4
5
6 837
7 838
8 839
9

Table 1 Average and standard deviation concentrations/activities of textural and potential fingerprinting properties measured in the soil sources and sediment core samples collected in the Kamech catchment and in its reservoir. Representativeness of each core in terms of sediment deposit volume in Kamech reservoir is also mentioned.

Fingerprint Properties		Number of samples	Clay [0-2 µm]	silt [2-50 µm]	sand [50-2000 µm]	²¹⁰ Pb-xs (Bq/Kg)	²¹⁰ Pb (Bq/Kg)	²³⁴ Th (Bq/Kg)	²²⁶ Ra (Bq/Kg)	²²⁸ Ra (Bq/Kg)	²²⁸ Th (Bq/Kg)	K (%)	¹³⁷ Cs (Bq/Kg)	TOC (%)	TN (%)	P_P ₂ O ₅ (%)	Core distance to the dam (m)	Core representativeness (%)
References		2	30.2	67.7	2.1	44.3	59.9	18.9	15.7	22.9	22	1	7.1	1.6	0.16	0.07		
			±	±	±	±	±	±	±	±	±	±	±	±	±	±		
			1.2	1.4	2.6	37.1	44.9	10.5	7.8	12.3	11	0.3	0.4	0.6	0	0		
Sources	Surface topsoil	8	36.3	62.8	0.9	6.1	29.3	28.1	23.3	39.8	38.5	1.4	3.7	1.1	0.15	0.15		
			±	±	±	±	±	±	±	±	±	±	±	±	±	±		
			6	5.9	0.6	6.1	4.1	7.1	5.8	10.6	10.2	0.3	1.5	0.1	0	0		
	Gully or channel bank	9	27.4	71.8	0.8	0.3	26.9	32.6	29.1	47.1	46.5	1.7	0.2	0.5	0.11	0.16		
			±	±	±	±	±	±	±	±	±	±	±	±	±	±		
			2.3	3.2	1	0.9	2.4	2.2	2.3	3.8	3.6	0.2	0.4	0.1	0	0		
Cores	C1	1*	34.3	65.5	0.2	24	51.3	37.6	27.5	52.2	53.6	1.9	3.4	0.89	0.16	0.17	63	30
	C2	1*	33.3	64.8	2	10.7	40	36.6	29.4	47.6	48.4	1.7	3	0.99	0.14	0.15	100	15.6
	C3	1*	30.3	68.2	1.4	10.9	37.3	35.4	26.5	49.1	49.9	1.7	3	1.1	0.16	0.16	137	10.7
	C4	1*	35.1	64.5	0.5	17.2	45.2	34	28.1	50.5	48.7	1.8	3.9	0.94	0.18	0.17	180	11.5
	C5	1*	29.6	69.2	1.2	9.8	37.2	35.8	27.5	47.8	47.8	1.7	2.9	1.21	0.16	0.15	220	8.3
	C6	1*	17.6	71.9	10.5	7.4	33.8	37.6	26.5	46.4	45.3	1.7	1.9	0.58	0.1	0.16	255	6.5
	C7	1*	18.6	66.9	14.5	7.6	35.5	32.7	28	45.6	44.4	1.5	1.6	0.84	0.12	0.14	275	4.1
	C8	1*	18.6	62.5	18.9	0	28.2	30.5	28.6	43.1	42.6	1.5	1.8	0.85	0.12	0.13	293	1.6
	C9	1*	18.2	74.4	7.4	3.3	26.2	26.6	22.9	39.9	39.6	1.4	1.2	0.61	0.1	0.15	304	4
	C10	1*	21	70.4	8.6	0	28.6	32.3	27.5	41	41.3	1.5	1.1	0.56	0.09	0.14	312	2.6
	C11	1*	17.4	71.8	10.9	3.7	28.5	34.1	24.9	42.5	42.6	1.5	0.9	0.52	0.09	0.16	332	1.4
	C12	1*	15.5	69.1	15.4	0	29.8	30.7	28.2	42.2	42	1.5	1.2	0.8	0.11	0.15	385	1
	C13	1*	10.8	55.8	33.4	0	31.2	33.9	29.8	45.2	46.1	1.6	1.1	1.1	0.14	0.16	449	2.7

* composite sediment sample

10
11
12
13
14
15
16
17
18
19
20
21
22
23
24
25
26
27
28
29
30
31
32
33
34
35
36
37
38
39
40
41
42
43
44
45
46
47
48
49

840

1
2
3
4
5
6
7
8
9
10
11
12
13
14
15
16
17
18
19
20
21
22
23
24
25
26
27
28
29
30
31
32
33
34
35
36
37
38
39
40
41
42
43
44
45
46
47
48
49
50
51
52
53
54
55
56
57
58
59
60
61
62
63
64
65

841 **Table 2** Results of the Kruskal-Wallis H-test applied to the eleven potential fingerprint properties measured for
842 the source soils collected in the Kamech catchment
843

Potential fingerprint	H-value
²¹⁰ Pb-xs (Bq.Kg ⁻¹)	5.79
²¹⁰ Pb (Bq.Kg ⁻¹)	0.75
²³⁴ Th (Bq.Kg ⁻¹)	8.33 *
²²⁶ Ra (Bq.Kg ⁻¹)	12.00 *
²²⁸ Ra (Bq.Kg ⁻¹)	8.33 *
²²⁸ Th (Bq.Kg ⁻¹)	9.48 *
K (%)	6.50
¹³⁷ Cs (Bq.Kg ⁻¹)	12.00 *
TOC (%)	11.34 *
TN (%)	5.56
P ₂ O ₅ (%)	3.89

844

845 * difference significant at p=0.05

846

847

848

849

850

851

1

2 852

3 853

4 854

5

6

Table 3 Results of the stepwise discriminate function analysis use to identify the optimum fingerprint property combination

<i>Fingerprint property added</i>	<i>Wilk's lambda</i>	<i>Cumulative % of samples classified correctly</i>
¹³⁷ Cs (Bq.Kg ⁻¹)	0.2247	77.53
C (%)	0.1123	100

13 855

14

15

16

17

18

19

20

21

22

23

24

25

26

27

28

29

30

31

32

33

34

35

36

37

38

39

40

41

42

43

44

45

46

47

48

49

50

51

52

53

54

55

56

57

58

59

60

61

62

63

64

65

856
1 857
2 858
3 859
4 860
5 861
6

Table 4 Basic statistics on the absolute errors in the source contribution evaluation for the three core sampling strategies. The absolute error is evaluated relative to the source apportionment for the entire reservoir as derived from the combined 13 cores with a weighting proportional to their representativeness in terms of sediment volume. The absolute error is calculated for each core as the absolute difference between surface contribution derived from the core and the one derived from the combined 13 cores.

Core sampling strategy	Absolute error (%)			
	Mean	Standard deviation	Minimum	Maximum
One core in downstream reservoir area (N = 5)	7.3	4.8	2.7	15.3
One core in upstream reservoir area (N = 8)	26.1	16.1	6.8	47.9
Two cores: one in downstream reservoir area with a 75% weighting and one in upstream reservoir area with a 25% weighting (N = 40)	4.1	3.1	0.2	9.9

16 862

17
18
19
20
21
22
23
24
25
26
27
28
29
30
31
32
33
34
35
36
37
38
39
40
41
42
43
44
45
46
47
48
49
50
51
52
53
54
55
56
57
58
59
60
61
62
63
64
65

Figure 1
[Click here to download high resolution image](#)

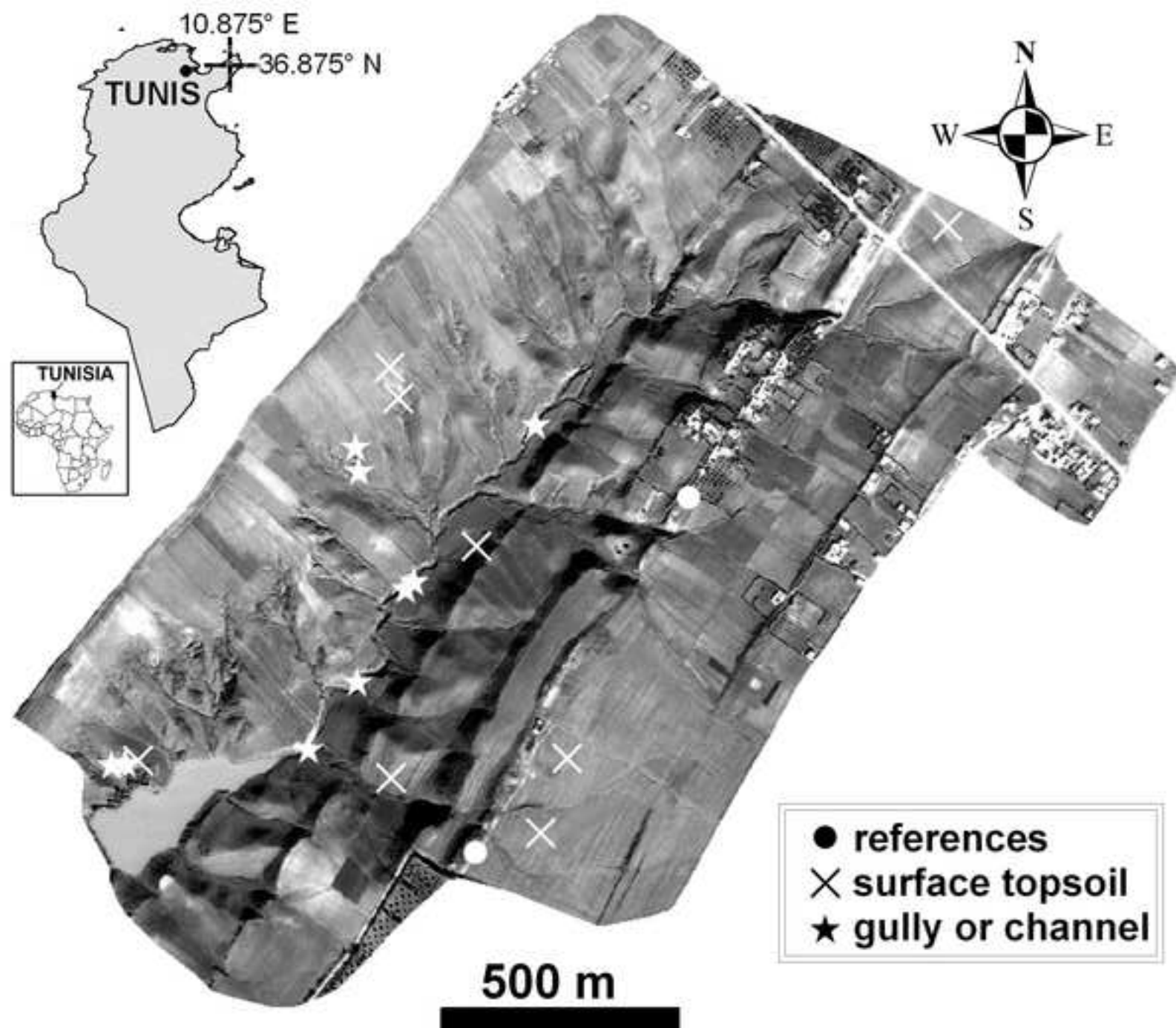


Figure 2
[Click here to download high resolution image](#)

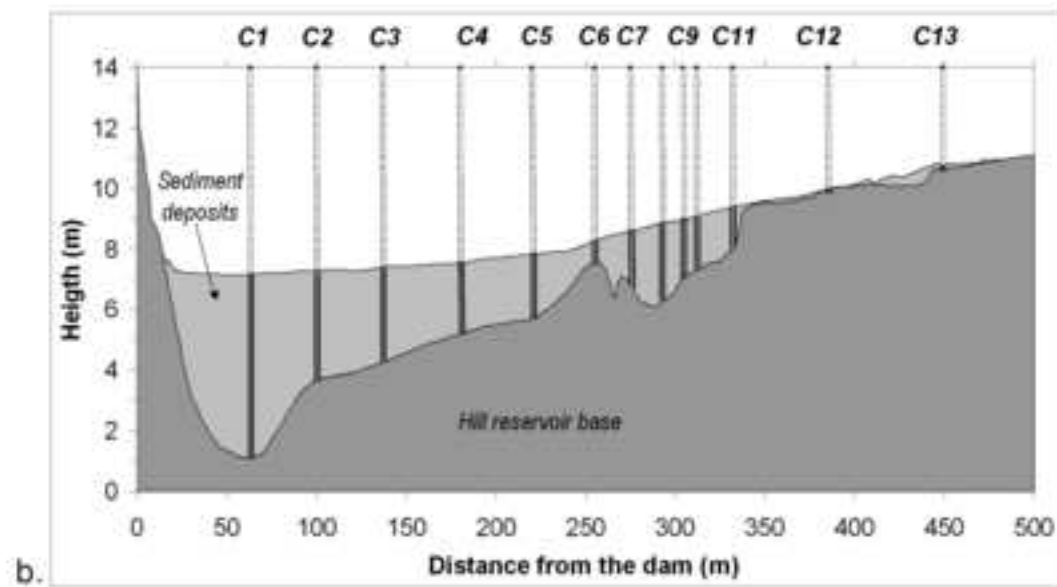
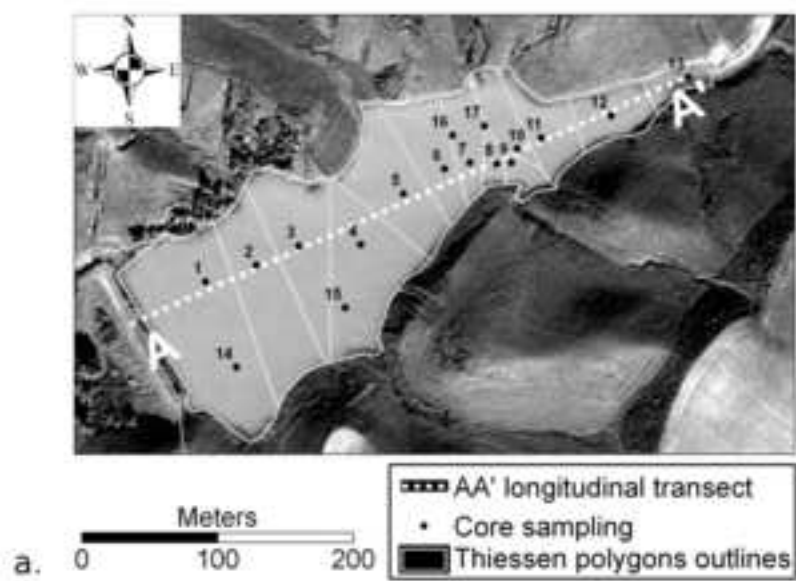


Figure 3
[Click here to download high resolution image](#)

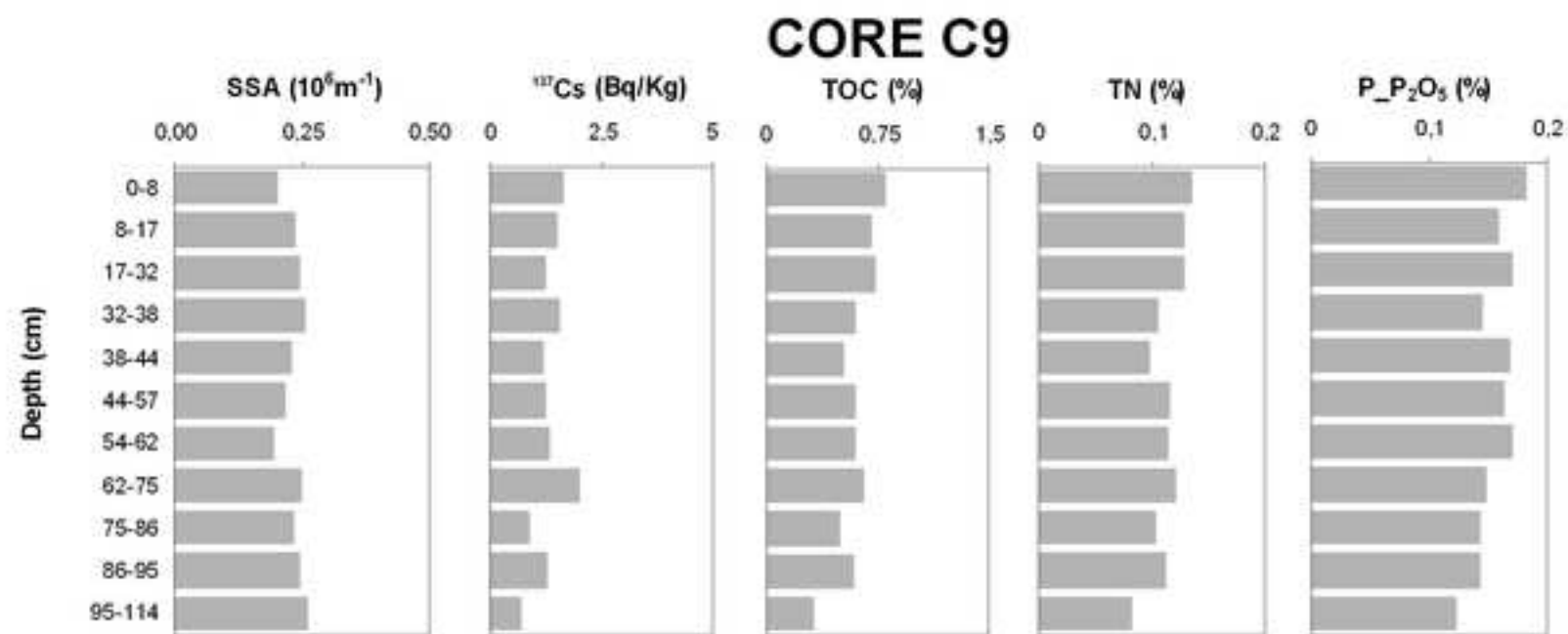
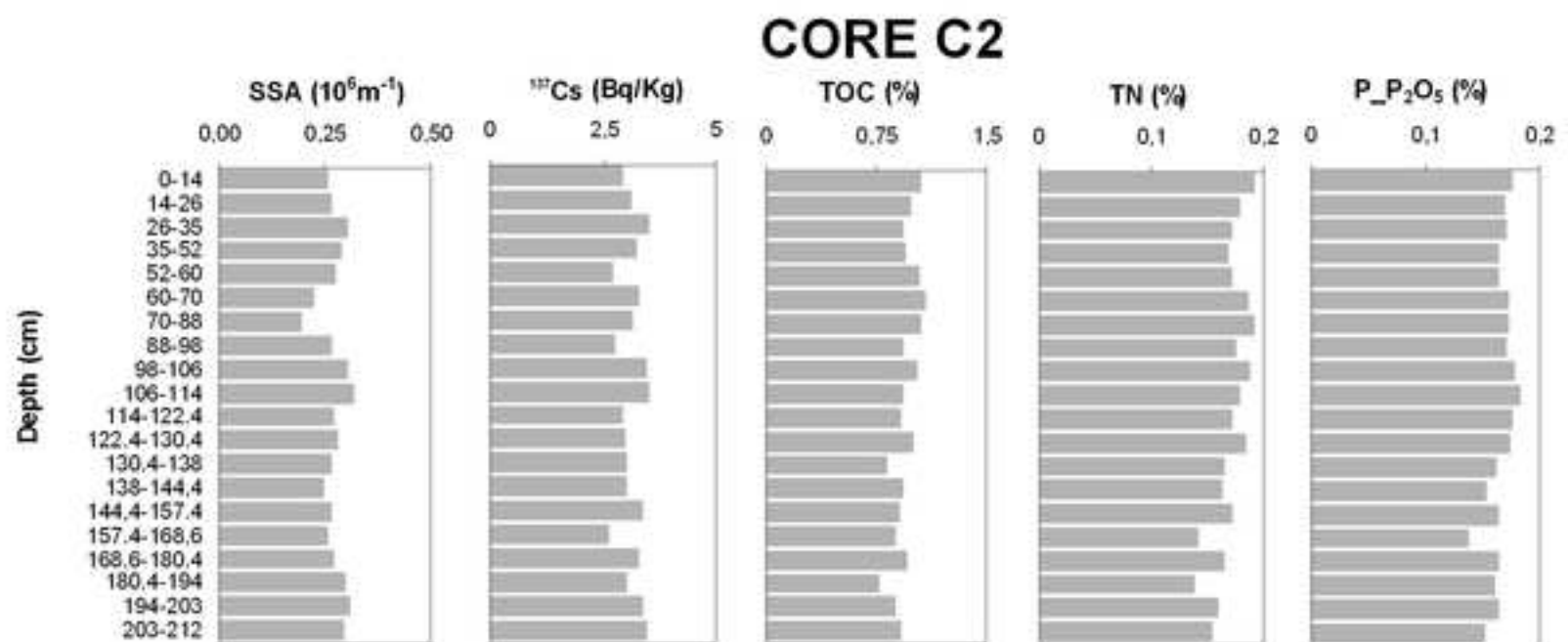


Figure 4
[Click here to download high resolution image](#)

Surface topsoil apportionment

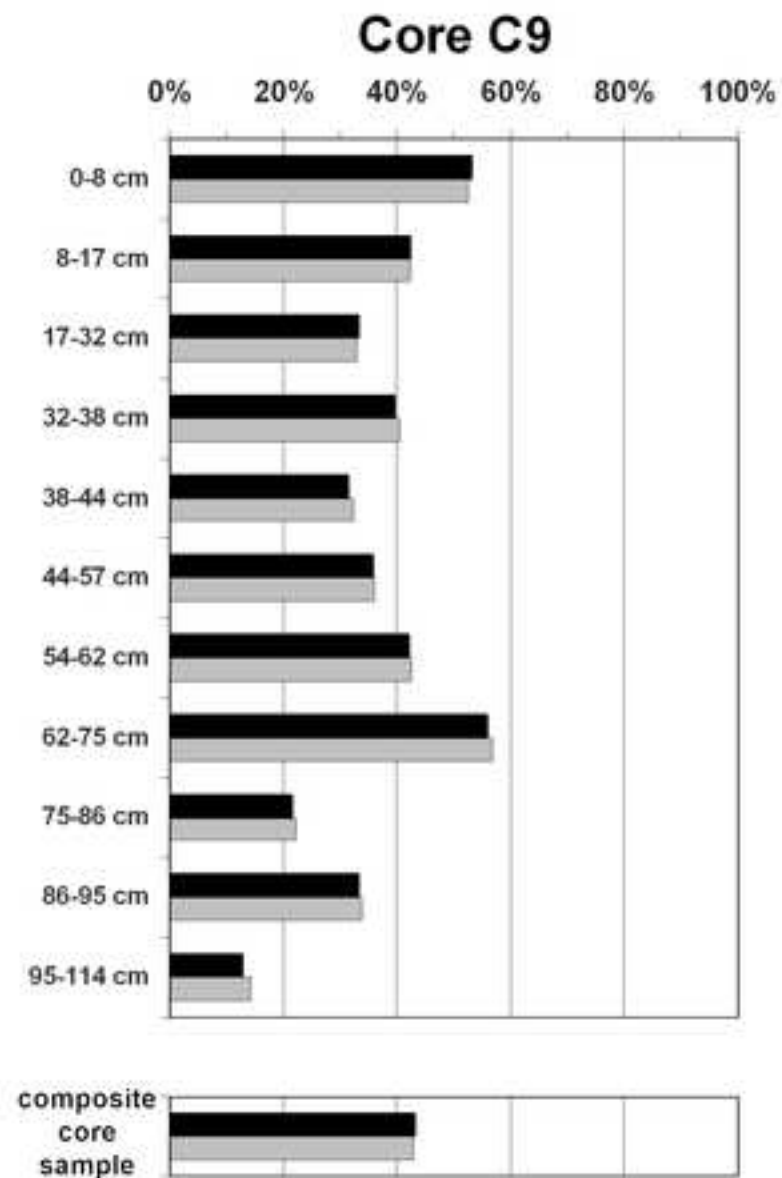
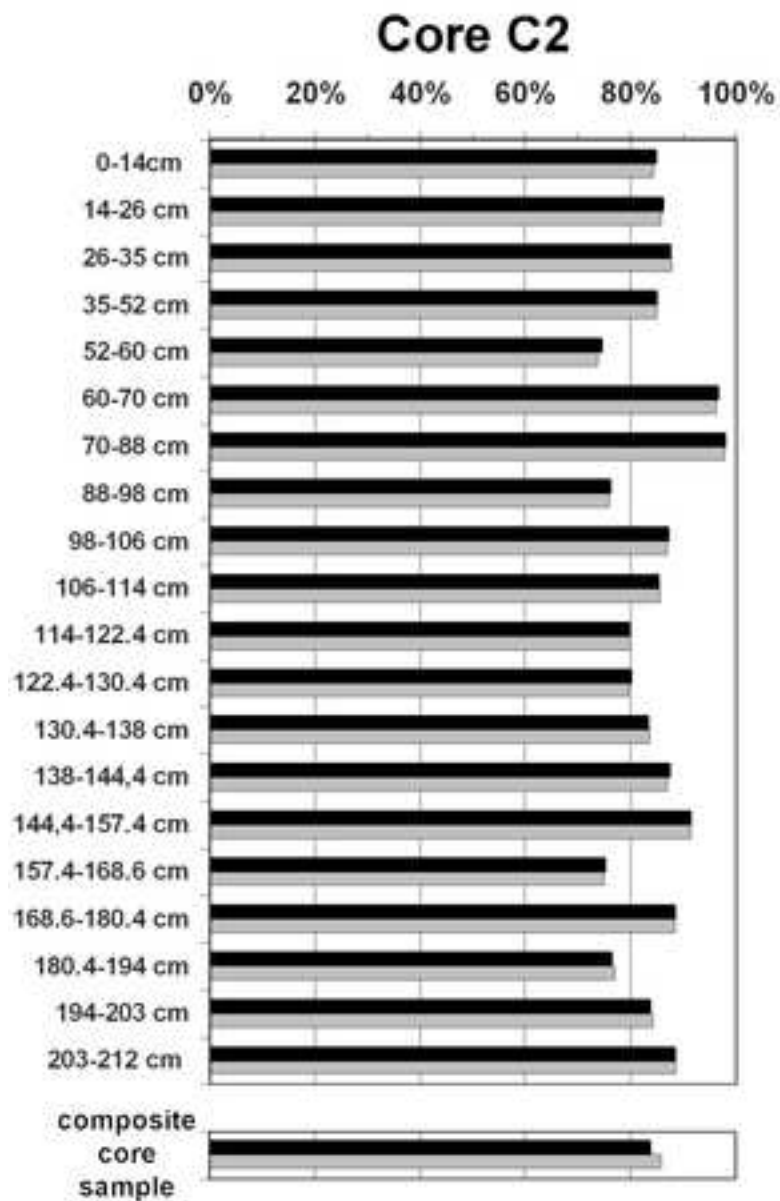
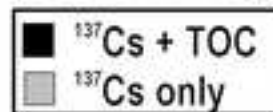


Figure 5
[Click here to download high resolution image](#)

Surface topsoil apportionment

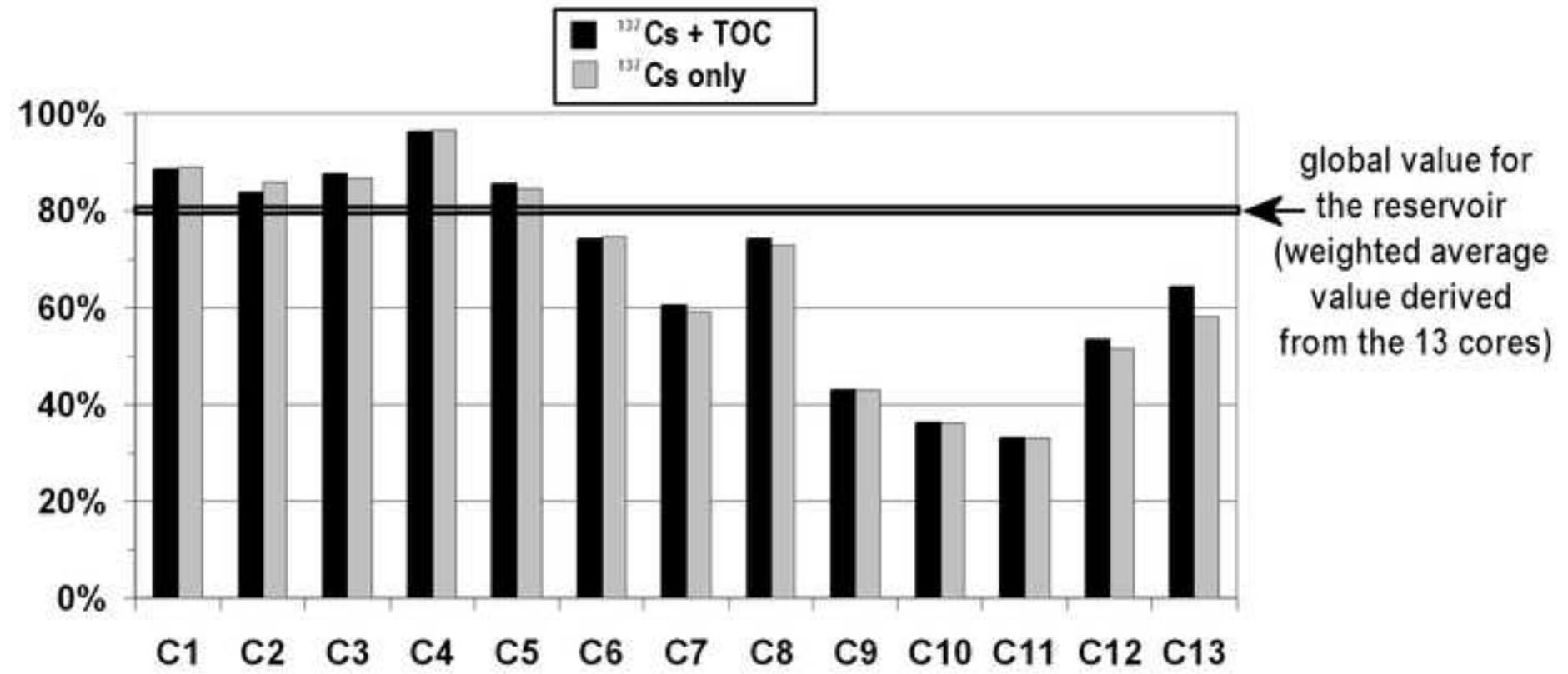


Figure 6
[Click here to download high resolution image](#)

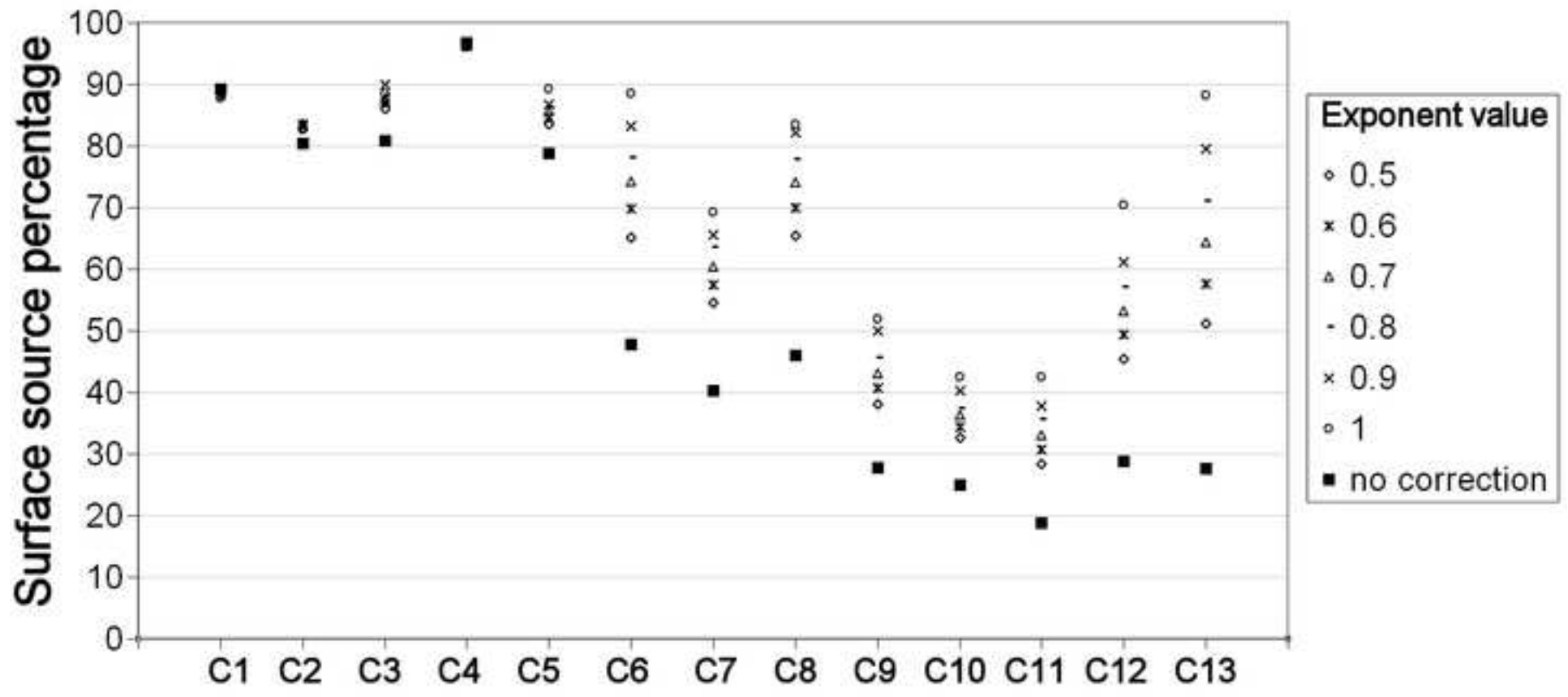


Figure 7

[Click here to download high resolution image](#)

